JOURNAL OF AIRCRAFT
Vol. 33, No. 2, March–April 1996

Critical States and Flow Structure on a 65-Deg Delta Wing

Charles E. Jobe,* Alexander H. Hsia,† Jerry E. Jenkins,‡ and Gregory A. Addington†
U.S. Air Force Wright Laboratory, Wright–Patterson Air Force Base, Ohio 45433

Swept and delta wings maneuvering at moderate and high angles of attack produce highly nonlinear and often discontinuous aerodynamic forces and moments that are difficult to model. The nonlinear indicial response (NIR) methodology and the concept of critical states accompanied by changes in the flow structure and topology could provide a rational framework for the analyses and modeling of these flows. The analysis of surface oil-flow photographs and laser light sheet high-speed video images of smoke flow has been performed. The correlation of the structural and topological changes in the flow with force and moment data follows. Critical states are often accompanied by changes in the flow topology and not all topological changes produce measurable changes in the forces and moments, however, a useful relationship may exist.

Introduction

AIRCRAFT with delta wings have flown since the early 1950s (Vulcan, F-102, Mirage III, MiG-21, B-58, XB-70, Eurofighter 2000 prototype, etc.), when the jet engine with its higher speed capability replaced propellers and piston engines. The drag reduction for thinner wings with increased sweep was well known and leads to the delta planform with greater structural rigidity, gradual stall characteristics, and high lift at maneuvering and landing attitudes and speeds. The triangular delta wing was, however, not without disadvantages that required stability augmentation and double-delta, straked delta, and other closely related planforms to correct. While primarily used for high-performance fighter aircraft, these planforms also have found application to the Concorde supersonic transport and proposed High Speed Civil Transport designs.

The nonlinear lift increase at low speeds is generated by leeward vortices produced by the rolling up of the shear layers emanating from the leading edges. These vortices, while producing the desirable lift increase, considerably complicate the flowfield and its prediction. The flowfield is symmetric and predictable at moderate angles of attack for symmetric flight conditions. Unpredictable changes in the static forces and moments occur during high angle-of-attack maneuvers and during even moderate asymmetric flight conditions when vortex burst may occur over the planform. Vortex burst or vortex breakdown is characterized by the sudden expansion of the highly organized core into bubbles or spirals along the core axis. Shortly downstream, the bubbles or spirals diffuse into a disorganized, swirling turbulent flow. Vortex burst normally occurs first in the wake, proceeding upstream toward the wing's apex as angle of attack, sideslip (windward wing only), or aspect ratio increase. Associated with the forward motion of the burst point are loss of lift, pitchup and nonlinear, often discontinuous, pitching and rolling moment characteristics.[1]

Beginning in 1987, the Canadian Institute for Aerospace Research (IAR) and the Flight Dynamics Directorate of Wright Laboratory have been pursuing a collaborative research program on unsteady and vortex-dominated flows. The need being addressed is the lack of appropriate mathematical modeling techniques to represent the interaction between the vehicle motion and the forces and moments created by these flows. The requirements for aerodynamic modeling arise in at least three areas: 1) for aerodynamic understanding and design, 2) for control system design, and 3) for flight simulation.

A theoretical method for studying the nonlinear aspects of the flight dynamics problem has been under development by Tobak and his colleagues[2–4] at NASA Ames Research Center since the early 1960s. Their approach introduced two important new concepts: 1) a nonlinear indicial response (NIR) and 2) a generalized superposition integral.

The NIR approach, which has been derived from the Navier–Stokes equations for a time-invariant equilibrium state,[4] allows that critical states may be signaled by changes in the static flow topology, often manifest in the position and behavior of vortices within the flow. The movement of the leading-edge vortex burst point onto the planform and the introduction of secondary and tertiary vortices are examples of topological changes, as are changes in the number of singular points in the skin-friction lines. In principle, the NIR is not restricted to a time-invariant equilibrium state; however, the details of the proof have not been completed and published.

As with linear indicial response methods, the arbitrary motion is represented as a summation of responses to a series of step motions. The NIR, as opposed to its linear counterpart, accounts for changes induced by the motion history leading up to step onset. Under a wide variety of circumstances, the summation of indicial responses approaches the generalized superposition integral in the limit.

The formulation also allows for critical states where the aerodynamic response loses analytical dependence on the motion variable, such as when aerodynamic bifurcations occur.[3] A critical state is accommodated by splitting the generalized superposition integral at the critical state and including a transient response term. Its location is defined by the values of a set of variables that characterize the instantaneous motion.

A critical state is a flight condition where large and persistent transients may be introduced into the aerodynamic loads, invalidating the linear and locally linearized aerodynamic models traditionally used for flight mechanics predictions. For example, the result of roll-angle and roll-rate-induced velocities at the leading edge of a delta wing is an unsymmetrical vortex lift that produces a highly nonlinear (perhaps discontinuous) change in the rolling moment.

A critical state is often associated with a change in the number of critical points in the static time-averaged surface flow

Presented as Paper 94-3479 at the AIAA Atmospheric Flight Mechanics Conference, Scottsdale, AZ, Aug. 1–3, 1994; received Sept. 7, 1994; revision received Oct. 11, 1995; accepted for publication Oct. 12, 1995.

*Aerospace Engineer, Building 146, Room 305, 2210 Eighth Street, Suite 11. Associate Fellow AIAA.

†Aerospace Engineer, Building 146, Room 305, 2210 Eighth Street, Suite 11. Member AIAA.

‡Aerospace Engineer, Building 146, Room 305, 2210 Eighth Street, Suite 11. Senior Member AIAA.

topology as shown later. Physically realizable flows produce streamlines and skin friction line patterns in oil flows that must satisfy topological rules based entirely on kinematics and the differential equations of streamlines. A stagnation point is a critical point, also called singular point and equilibrium point,[5] in the flow as is a point where the skin friction vector is zero. Critical points are classified as nodes or saddles depending on their appearance and mathematical properties. Nodes are further subdivided into nodal points of attachment or separation, foci, and centers. All skin-friction lines or streamlines intersect at the node and are directed away from a node of attachment and toward a node of separation. The focus or spiral node has all of the lines spiraling inward or outward around the critical point. If the trajectories form closed paths around the focus, it is a center. The saddle has two oppositely directed lines that intersect at the critical point. All other lines curve away in each quadrant to avoid this critical point.

The correspondence between critical states and static flow topology changes is controversial, especially when time-averaged data (e.g., surface oil flow studies) are involved (see Ref. 6). The analytic dependence of the aerodynamic response may be lost at a change in flow topology, i.e., when a change in the number of critical points is observed.[3] A current consensus is that critical states are often signaled by changes in the flow topology; however, some changes in the flow topology do not produce measurable force and moment transients. A complete discussion of the controversy and how vortex formation in the wake of a circular cylinder at low Reynolds number provides a counterexample has been given by Jenkins et al.[6]

Experimental Program

The flow about delta wings is highly sensitive to very small differences in model geometry, motion variables, and flow conditions making analysis and correlation of the vast amounts of available data difficult. The experimental program eliminated many of these variables by testing the same model in two wind tunnels at similar flow conditions with overlapping ranges of the motion variables and different support systems. The program is continuing with previous measurements identifying regions of particular interest for succeeding tests.

The common model is a 65-deg swept triangular wing with sharp leading edges (10-deg symmetric nonconical bevel on all three edges) and centerbody (Fig. 1). It was especially designed and constructed to be lightweight, with low inertia to attain the desired motions, yet strong enough to withstand the loads encountered at the high pitch and roll rates required to match full-scale aircraft reduced frequencies (see Hanff and Jenkins[7] for details).

Static and dynamic tests of this model have been a particularly rich source of nonlinearities and other unusual dynamic behavior. The extensive experimental database allows concurrent study of vortex dynamics and the resulting unsteady aerodynamic forces and moments. The correct identification of changes in the flow physics and topology is crucial to further understanding the NIR methodology and its application to this series of wind-tunnel test data.

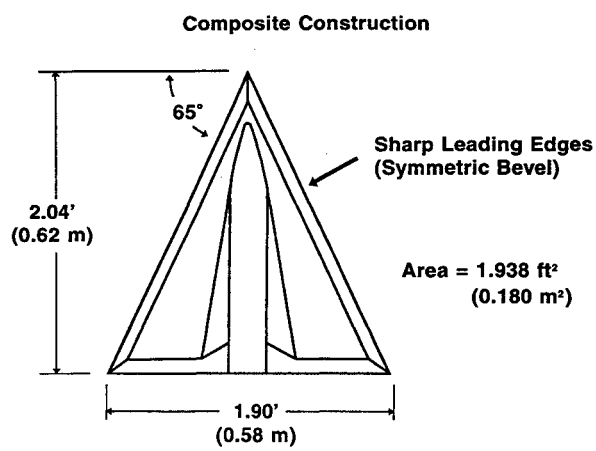

Fig. 1 Model geometry.

The IAR experimental program, conducted in the National Aeronautical Establishment 6 × 9 ft low-speed wind tunnel, has been described by Hanff and Jenkins[7] and Huang et al.[1] The Wright Laboratory 7 × 10 ft Subsonic Aerodynamic Research Laboratory and the experimental data has been described by Jenkins and various coauthors.[6,8,9] IAR personnel conducted all dynamic testing using their roll rig. The most extensive data set was taken at Mach number 0.3, Reynolds number 3.6×10^6 based on the centerline chord of 2.04, (0.622 m) sting angle of 30 deg, with various static and mean roll angles ϕ, and roll rates. The static roll response is highly nonlinear,[10] with three distinct static roll attractors. Further, forced-oscillation and free-to-roll data exhibited strong nonlinearities that cannot be modeled using locally linear models.[6]

Critical States and Topology

Analysis of the static and dynamic force and moment data[6] indicated critical states near $\phi = 5$ and 11.3 deg, based on slope changes and discontinuities in the static time-averaged pitching and rolling moments and transients in the dynamic data. Additional evidence confirming the existence of these critical states has been provided by a wealth of subsequent experimental data[8,9] and analyses.[1,11] The following analysis correlates the changes in static forces and moments with the topology changes described by Huang et al.[1] The changes in the forces are small because the vortex flow patterns contribute

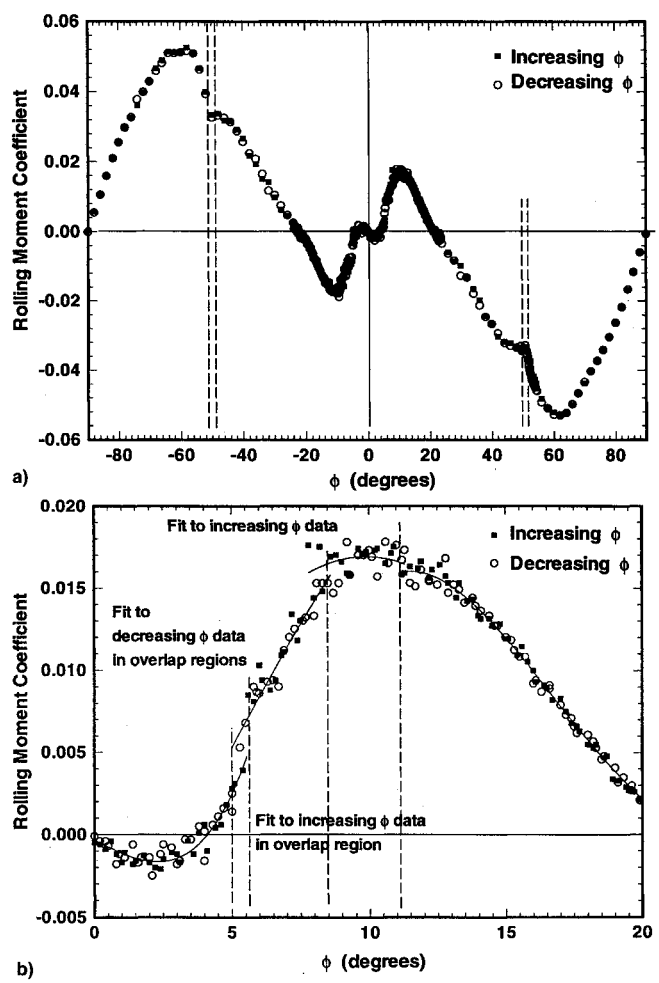

Fig. 2 Rolling moment coefficient: a) full range, $-90 \leq \phi \leq 90$ deg and b) expanded scale, $0 \leq \phi \leq 20$ deg.

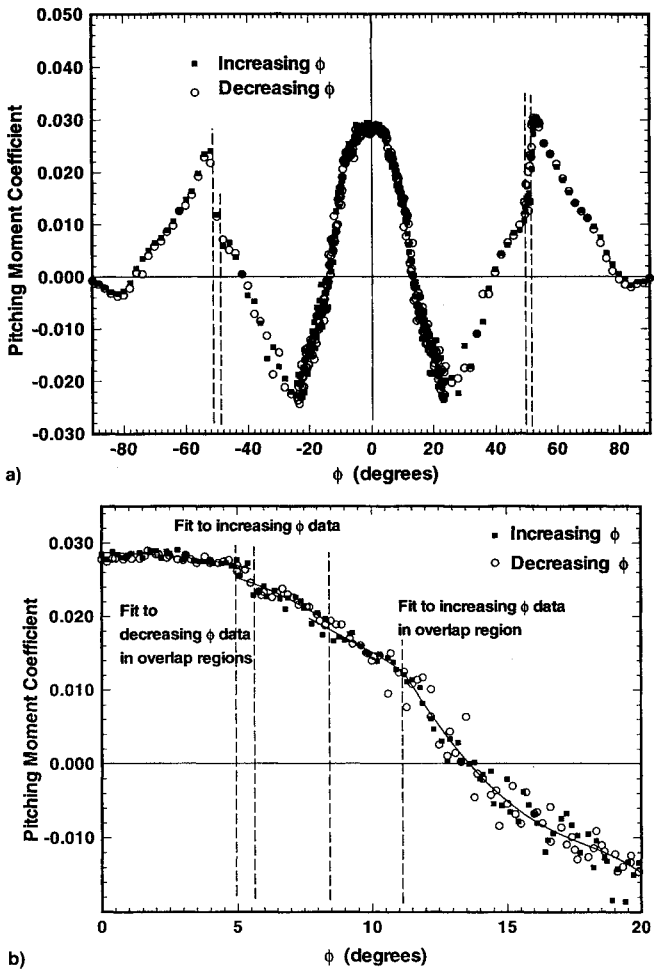

Fig. 3 Pitching moment coefficient: a) full range, $-90 \leq \phi \leq 90$ deg and b) expanded scale, $0 \leq \phi \leq 20$ deg.

less than 10% of the total lift at 30-deg angle of attack, zero roll angle for this aspect ratio 1.86 wing. Thus, changes in the vortex flows rarely obviate trends established by the attached flow, as will be discussed subsequently. Critical states, however, lead to large deviations from the static characteristics, especially in the moments.

Experimental data for the entire roll angle range (-90 to $+90$ deg) and to an expanded scale emphasizing the 5 and 11.3 deg (to be discussed later) critical states are shown in Figs. 2–5. The force and moment coefficients are based on the dynamic pressure and the wing area of 1.94 ft^2 (0.180 m^2). Reference lengths are the mean aerodynamic chord of 1.36 ft (0.415 m) for the pitching moment coefficient and the wing span of 1.90 ft (0.58 m) for the body-axis rolling moment coefficient. Dashed vertical lines indicate the critical state locations. The data has been sorted and plotted according to the direction the wing was rolling toward (increasing or decreasing ϕ) when the particular roll angle was attained. This is contrary to previous analyses[6,8,9] based on rather sparse static data and permits a more detailed examination for discontinuities, slope changes, and hysteresis that indicate the crossing of critical states.

The full-range data plots, Figs. 2a, 3a, 4a, and 5a, show proper symmetry. Time-averaged force and moment behavior at the previously determined critical states at large roll angles[9] (-51.3, -49.5, 50.1, and 51.4 deg), are also shown on these figures as dashed vertical lines. The data density on this scale precludes definite identification of the critical states at either $\phi = 5$ or 11.3 deg. All data were fit using Legendre polynomials and stepwise regression analysis as reported previously[6,9] on the earlier sparse data sets.

Five-Deg Critical State

The discontinuity near 5-deg roll angle in Figs. 2b, 3b, and 4b is clearly a critical state. It is associated with the leeward (port for positive roll angles) wing vortex burst rapidly crossing the trailing edge during extremely small roll angle increases, as shown by previous authors.[6,8,9] This is in agreement with the topological maps of Huang et al.[1] that show the primary vortex burst is over the leeward wing at $\phi = 4$ deg and is absent at $\phi = 7$ deg. It is only the secondary and tertiary vortices that lift off [shown as whorls or foci (spiral nodes) in the skin-friction topology] at $\phi = 7$ deg.

Figure 6a shows the vortex burst of the leeward leading-edge vortex is 10–15% chord aft of the trailing edge at $\phi = -5.4$ deg, while Fig. 6b shows the vortex burst has moved upstream onto the planform at $\phi = -5.0$ deg. Note the rapid forward progression to 10–15% chord ahead of the trailing edge in only 0.4-deg roll angle change. This is the discrete change that defines the critical state.

The increase in positive rolling moment as ϕ increases (Fig. 2b) is consistent with the formation of the coherent vortex over the entire leeward wing. As the vortex burst point moves aft, off the wing, the extended, concentrated vortex core decreases the pressures on the leeward wing upper surface and contributes an additional destabilizing moment. The additional force near the trailing edge also contributes a nose-down, stabilizing increment to the pitching moment (Fig. 3b). The axial force (Fig. 4b) shows an increase, consistent with the known drag increase attendant with lifting leading-edge vortices. The normal force is decreasing because of the sideslip increase.

The regression analysis performed on data in this region was split into two separate domains, increasing and decreasing ϕ,

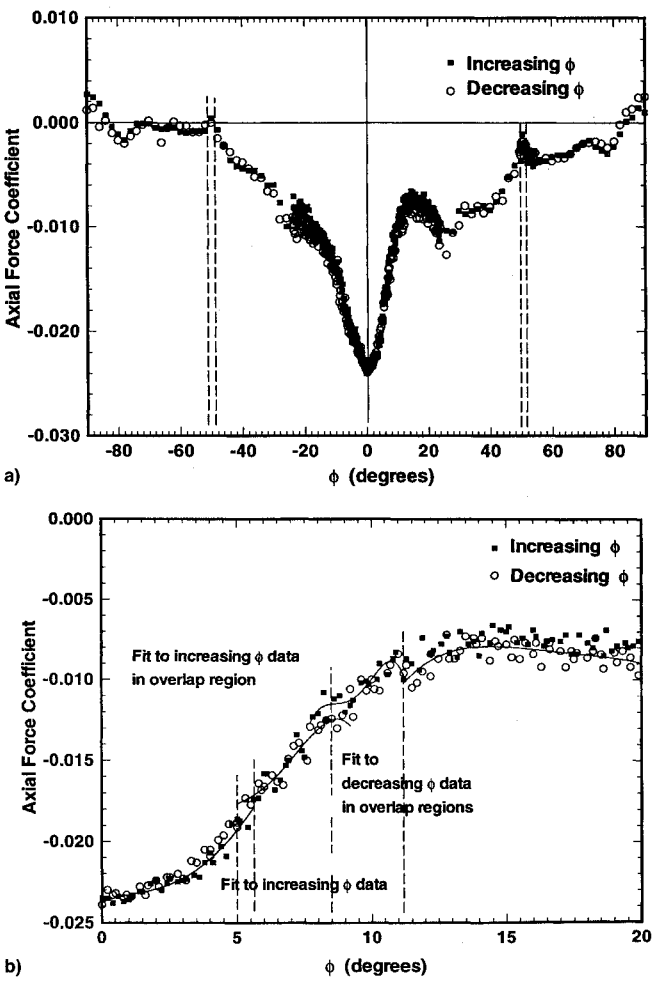

Fig. 4 Axial force coefficient: a) full range, $-90 \leq \phi \leq 90$ deg and b) expanded scale, $0 \leq \phi \leq 20$ deg.

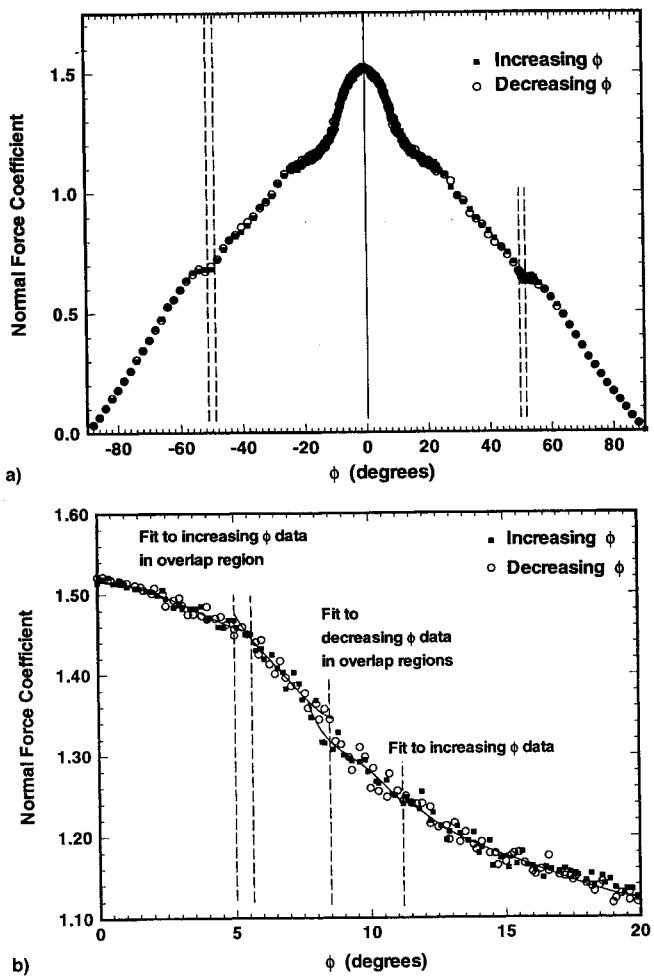

Fig. 5 Normal force coefficient: a) full range, $-90 \leq \phi \leq 90$ deg and b) expanded scale, $0 \leq \phi \leq 20$ deg.

between $\phi = 5.0-5.7$ deg. Only the increasing ϕ data were used in this region for the regression fitting the lower branch in this region, while only decreasing ϕ data were used for the upper branch. This partitioning of data is consistent with the definition of a static hysteresis, and shows that a narrow hysteresis loop apparently exists in this region. Further, two critical states must exist here, one at the terminus of each branch. Past and present analyses of experimental data suggest such a possibility. The analysis of Addington and Jenkins[8] show that the leeward leading-edge vortex burst point crosses the trailing edge from being over the planform at approximately $\phi = 5$ deg. Huang et al.[1] analysis confirms this finding, as well as suggests that an additional topological change occurs in this region.

Several correlations have been devised to predict the movement of vortex burst points with leading-edge sweep angle, angle of attack, and roll angle. The predicted roll angle for vortex breakdown at the trailing edge is 7 deg based on a linear regression fit[8] of the static data of Hanff and Huang[12]; 8.8 deg based on Ericsson and Hanff's[10] method (using Wentz and Kohlman's[13] vortex breakdown correlations, vortex breakdown occurs at the trailing edge at 19-deg angle of attack for $\phi = 0$ deg); and 13.7 deg from the revised Huang and Hanff[14] method. Their correlations are a better approximation to experimental data[11,14] for the 60- and 70-deg swept wings than for the 65-deg swept wing, again indicating unusual behavior[9,10] at this combination of roll and sweep angles. None of these vortex breakdown prediction methods account for the rapid jump in vortex position because they assume smooth functions to correlate the experimental data.

11.3-Deg Critical State

The tentatively associated change in flow topology near $\phi = 12$ deg, the vortex breakdown point reaching the windward (starboard) wing's apex,[6] was shown to be erroneous[8] by analysis of the subsequent static and forced-oscillation dynamic wind-tunnel data called for by Jenkins et al.[6] The assumption of vortex breakdown reaching the apex of the windward wing near $\phi = 12$ deg was not unfounded, particularly in light of the lack of detailed flow visualization data available at the time. The linear regression data fit of Addington and Jenkins[8]

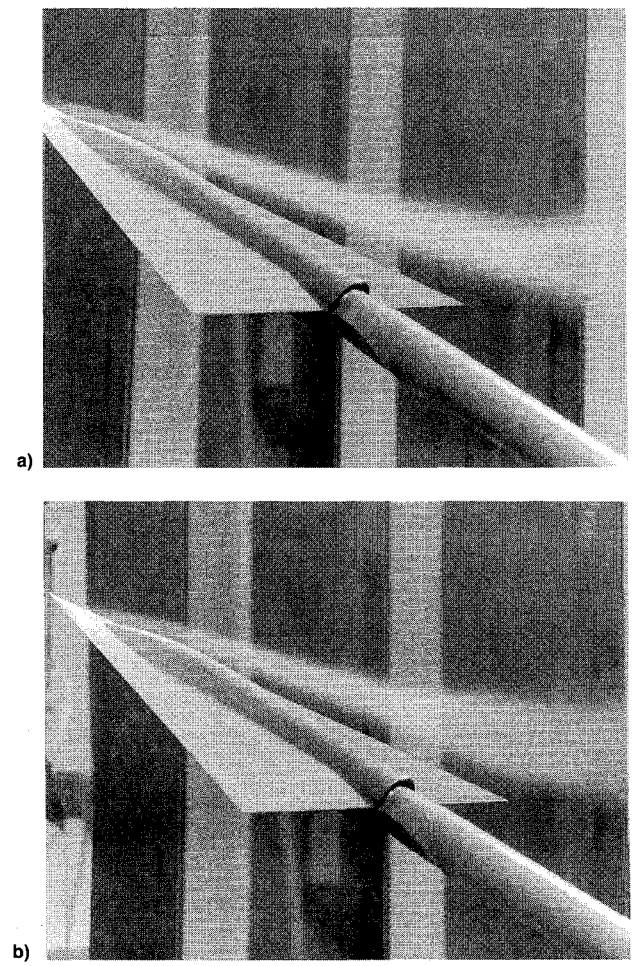

Fig. 6 Leeward leading-edge vortex burst: a) in the wake, $\phi = -5.4$ deg and b) over the planform, $\phi = -5.0$ deg.

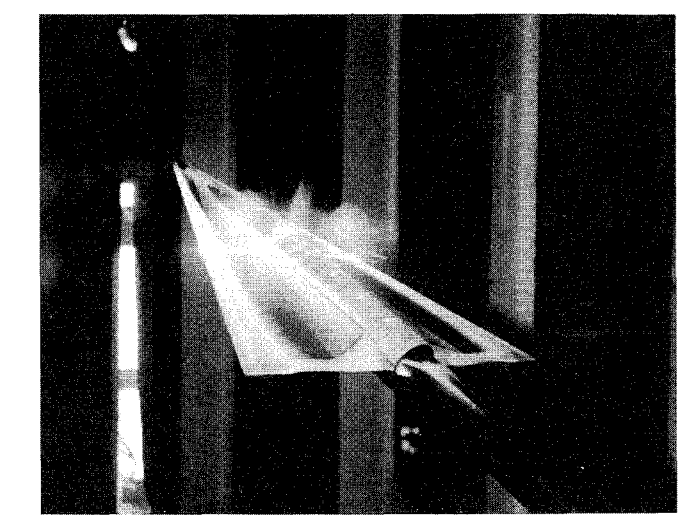

Fig. 7 Laser light sheet flow visualization.

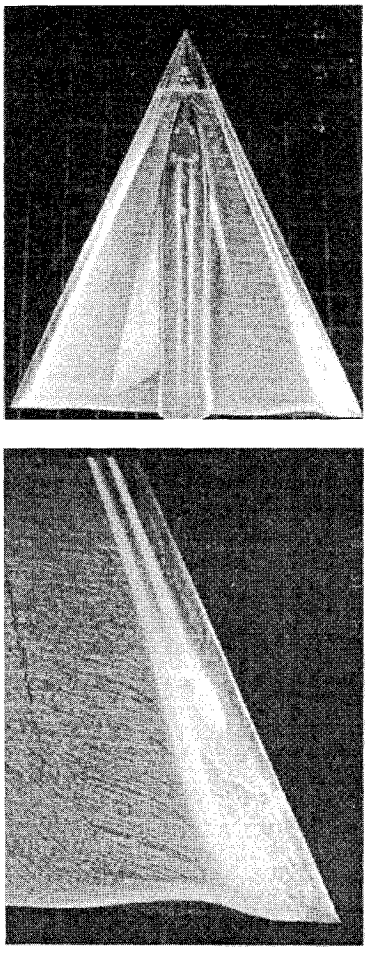

Fig. 8 Surface oil flow, $\phi = -7$ deg.

predicted $\phi = 13$ deg, whereas the methods of Ericsson and Hanff[10] and Huang and Hanff[14] predicted 12.6 and 12.15 deg, respectively. Vortex breakdown would occur aft of the trailing edge on the leeward wing and could not cause the observed force and moment transients. The preceding analysis methods generally agree with the original association of vortex breakdown at the apex. However, analysis of the previous dynamic and new high-resolution static data taken in the same wind tunnel using the same model (the sting and instrumentation were different, which permitted additional verification of the data through correlations at selected tie-in conditions) clearly shows that the critical state is not associated with vortex breakdown advancing to the apex at $\phi = 11.3$ deg.

The experimental setup with the laser light sheet is shown in side view in Fig. 7. The laser light sheet has progressed to aft of the midchord and the leading-edge vortex over the entire leeward wing is evident at $\phi = 14.5$ deg. The light sheet shows the shear layer from the windward wing has moved across the centerbody at this chordwise station, in agreement with the observations of Hsia et al.[9] Video recordings of the fore and aft sweeps of the laser light sheets show that the flow becomes unsteady as the critical roll angle is approached and returns to steady motion as this roll angle is exceeded. While a still image suitable for publication could not be captured by our equipment, the videotapes clearly show a vortex near the apex of both the windward and leeward wings at $\phi = 15$ deg. Both vortices are evident at all roll angles less than 15 deg, while the vortex over the windward wing is not apparent at $\phi = 18$ deg. The vortex persists over the entire leeward wing at this roll angle.

Surface oil flows near the trailing edge at nearly the same test conditions (30-deg roll angle and 0.3 Mach number) are shown in Figs. 8 and 9 at roll angles of -7 and -14 deg. A description of the model and experimental setup is contained in Hanff et al.[15] The change in flow topology is evident. Two vortex whorl patterns are evident over the leeward wing at a roll angle of -7 deg, while one is evident at $\phi = -14$ deg. These patterns correspond to the liftoff of the tertiary vortex (Fig. 8) and to liftoff of both the secondary and tertiary vortices (Fig. 9) on the planform. The flow pattern and topology sketches from Huang et al.[1] show this topology change occurs between roll angles of -7 and -14 deg, but the precise roll angle and triggering mechanism are unknown. According to Huang et al.,[1] the change in flow pattern corresponds to a critical state crossing; however, additional images and analysis are needed to fill these experimental data gaps.

From Huang et al.,[1] between 10- and 14-deg roll angle, the flow on the windward wing changes from an organized vortex flow with the tertiary vortex lifting off the surface to a topology representative of primary vortex breakdown advancing toward, but not attaining, the wing apex. This creates a disorganized spiraling flow aft of the breakdown, exhibiting reverse flow partly swept across from the leeward wing, and a loss of vortex lift on the windward wing. The leeward wing undergoes a topological change indicative of reattachment of the secondary vortex near the wingtip as the roll angle increases. The organized, spiraling flow beneath this secondary vortex increases the normal force on the area near the wingtip and produces force and moment changes similar to the 5-deg case, albeit smaller. The force and moment changes are also influenced by the vortex lift loss over the windward wing.

Returning to Figs. 2–5, at $\phi = 11.3$ deg, the negative slope of the rolling moment curve becomes less negative because of the additional destabilizing moments contributed by both the windward and leeward wings (Fig. 2b). The nose-up pitching moment slope is increased by the additional force near the leeward wing trailing edge (Fig. 3b), causing the discontinuity in slope. The scatter in the axial force data (Fig. 4b) and the magnitude of the changes precludes definitive conclusions;

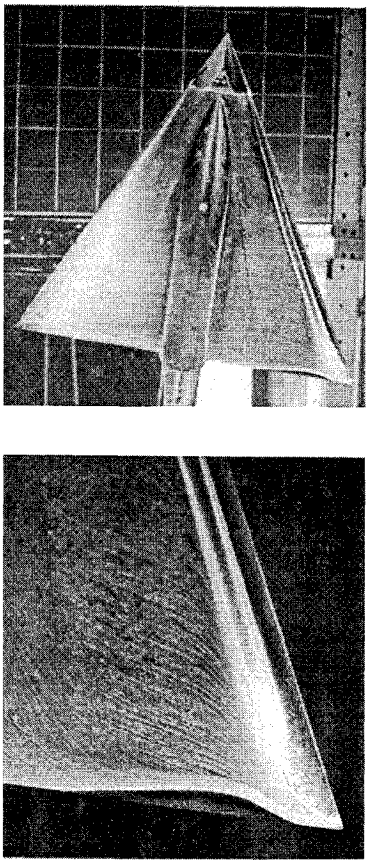

Fig. 9 Surface oil flow, $\phi = -14$ deg.

however, a discontinuity in slope is evident. The overall normal force is decreasing (Fig. 5b) because of increasing roll angle and the additional force caused by the leeward vortex is somewhat counteracted by the reduced vortex lift over the windward wing. The rate of lift decrease is slowed and causes the slope discontinuity.

8.5-Deg Critical State

A suspected critical state is marked at $\phi = 8.5$ deg in Figs. 2b–5b. The topological change shown by Huang et al.[1] reinforces the evidence obtained by separately fitting the roll angle increasing or decreasing data.

The polynomial regression fit of the experimental force and moment data for increasing and decreasing roll angle is shown as solid lines in Figs. 2b, 3b, 4b, and 5b. Two distinct branches near $\phi = 8.5$ deg are evident in each data set. The use of an overlapping domain (from $\phi = 7.7$ to 9.2 deg) to fit the data increases the correlation coefficient compared to strictly monotonic data fits.

Huang et al.[1] report that a topology change occurs between $\phi = 7$ and 10 deg. This change is associated with global flow separation occurring over the windward (starboard) wing as roll angle increases. The force and moment discontinuities occurring; increase in rolling moment, decrease in nose-up pitching moment, and decrease in axial and normal forces are consistent with the loss of suction because of the disappearance of the leading-edge vortex over the windward wing.

Discussion

The previous correlations agree with the topological analysis of Huang et al.[1] that is based on oil flow pictures and video images taken at discrete roll angles every 3 or 4 deg. Additional anomalies in the force and moment data create the possibility of additional topological changes. The separate analysis of roll angle increasing or decreasing data indicates the possibility of hysteresis at the 5-deg critical state (Fig. 2b) that would require two critical states, one near 5.0 deg and one near 5.7 deg. Hysteresis is also evident in the pitching moment data (Fig. 3b) and an additional discontinuity appears near $\phi = 8$ deg, where flow visualization data were not recorded.

A presently unexplained anomaly appears in these data. The branches in the force and moment data at $\phi = 8.5$ deg cannot form a hysteresis loop. The increases or decreases in the coefficients are either in the opposite direction or at opposite ends of where they would occur in a hysteresis loop. Furthermore, only one topology change is observed between $\phi = 7-10$ deg in the mean surface oil flows. The lack of data in this roll angle range does not permit resolution of this anomaly, however, several possible explanations are 1) additional topological changes occur in the surface flow, 2) topological changes occur in the streamlines of the off-body flow, or 3) the flow becomes unsteady through a Hopf bifurcation.

Current analyses are based on surface oil flows related to static force and moment data. The time-averaging property of this flow visualization method precludes inference of the unsteady effects necessary to further elucidate the relationship between critical states in the aerodynamic response and changes in the number of critical points in the flow.

Certainly a wealth of interesting possibilities occurs that cannot be confirmed based on presently available data, but point to the need for specific high resolution data to resolve these questions. The high resolution available from Navier–Stokes numerical simulations[16] of these experiments cannot be equaled for directing attention to, and clarifying, otherwise confusing or unnoticed flow features. It is currently too expensive to perform simulations at all of the points needed. The need for additional testing to fill these gaps is evident.

Correlation of critical states and topology changes is exceedingly difficult and time consuming because of the precision and resolution required in both the static and dynamic data. The static force and moment data across suspected discontinuities and hysteresis loops should be used, along with flow visualization, to identify conditions for critical states. Subsequent dynamic experiments should focus on these conditions to identify critical-state transient characteristics.

Acknowledgments

This work was conducted under a Joint Research Program of the U.S. Air Force Office of Scientific Research, their support is gratefully acknowledged as are the efforts of the Canadian Institute of Aerospace Research personnel.

References

[1]Huang, X. Z., Hanff, E. S., Jenkins, J. E., and Addington, G., "Leading-Edge Vortex Behavior on a 65° Delta Wing Oscillating in Roll," AIAA Paper 94-3507, Aug. 1994.

[2]Tobak, M., and Pearson, W. E., "A Study of Nonlinear Longitudinal Dynamic Stability," NASA TR R-209, Sept. 1964.

[3]Tobak, M., Chapman, G. T., and Unal, A., "Modeling Aerodynamic Discontinuities and Onset of Chaos in Flight Dynamical Systems," Annales Des Telecommunications, Vol. 42, Nos. 5–6, 1987, pp. 300–314; also NASA TM-89420, Dec. 1986.

[4]Truong, K. V., and Tobak, M., "Indicial Response Approach Derived from Navier-Stokes Equations Part 1, Time Invariant Equilibrium State," NASA TM 102856, Oct. 1990.

[5]Kaplan, W., *Ordinary Differential Equations*, 1st ed., Addison–Wesley, Reading, MA, 1958, pp. 414–470.

[6]Jenkins, J. E., Myatt, J. H., and Hanff, E. S., "Body-Axis Rolling Motion Critical States of a 65-Degree Delta Wing," AIAA Paper 93-0621, Jan. 1993.

[7]Hanff, E. S., and Jenkins, S. B., "Large-Amplitude High-Rate Rolling Experiments on a Delta and Double Delta Wing," AIAA Paper 90-0224, Jan. 1990.

[8]Addington, G., and Jenkins, J., "Flow Visualization of a Rolling Delta Wing and Its Pertinence to the Nonlinear Indicial Response Model," AIAA Paper 93-3469, Aug. 1993.

[9]Hsia, A. H., Myatt, J. H., and Jenkins, J. E., "Nonlinear and Unsteady Aerodynamic Responses of a Rolling 65-Delta Wing," AIAA Paper 93-3682, Aug. 1993.

[10]Ericsson, L., and Hanff, E. S., "Further Analysis of High-Rate-Rate Rolling Experiments of a 65 Deg Delta Wing," AIAA Paper 93-0620, Jan. 1993.

[11]Huang, X. Z., and Hanff, E. S., "Prediction of Leading-Edge Vortex Breakdown on a Delta Wing Oscillating in Roll," AIAA Paper 92-2677, June 1992.

[12]Hanff, E. S., and Huang, X. Z., "Roll-Induced Cross-Loads on a Delta Wing at High Incidence," AIAA Paper 91-3223, Sept. 1991.

[13]Wentz, W. H., and Kohlman, D. L., "Vortex Breakdown on Slender Sharp-Edged Wings," *Journal of Aircraft*, Vol. 8, No. 3, 1971, pp. 156–161.

[14]Huang, X. Z., and Hanff, E. S., "Prediction of Normal Force on a Delta Wing Rolling at High Incidence," AIAA Paper 93-3686, Aug. 1993.

[15]Hanff, E. S., Kapoor, K., Anstey, C. R., and Prini, A., "Large-Amplitude High-Rate Roll Oscillation System for the Measurement of Non-Linear Airloads," AIAA Paper 90-1426, June 1990.

[16]Chaderjian, N., and Schiff, L., "Navier-Stokes Prediction of Large-Amplitude Forced and Free-to-Roll Delta Wing Oscillations," AIAA Paper 94-1884, June 1994.